JOURNAL OF VIROLOGY, Apr. 2008, p. 3642–3653 Vol. 82, No. 7
0022-538X/08/$08.00+0 doi:10.1128/JVI.02409-07
Copyright © 2008, American Society for Microbiology. All Rights Reserved.

# Selective Ablation of Virion Host Shutoff Protein RNase Activity Attenuates Herpes Simplex Virus 2 in Mice[▽]

Maria Korom, Kristine M. Wylie, and Lynda A. Morrison*

*Department of Molecular Microbiology and Immunology, Saint Louis University School of Medicine, 1100 S. Grand Blvd., St. Louis, Missouri 63104*

Received 7 November 2007/Accepted 16 January 2008

**The virion host shutoff (vhs) protein of herpes simplex virus (HSV) has endoribonuclease activity and rapidly reduces protein synthesis in infected cells through mRNA degradation. Herpes simplex virus 1 (HSV-1) and HSV-2 vhs mutants are highly attenuated in vivo, but replication and virulence are largely restored to HSV-2 vhs mutants in the absence of a type I interferon (IFN) response. The role of vhs in pathogenesis and the hindrance of the type I IFN response have classically been examined with viruses that completely lack vhs or express a truncated vhs protein. To determine whether RNase activity is the principal mechanism of vhs-mediated type I IFN resistance and virulence, we constructed a HSV-2 point mutant that synthesizes full-length vhs protein lacking RNase activity (RNase$^-$ virus). Wild-type and mutant HSV-2 vhs proteins coimmunoprecipitated with VP16 and VP22. vhs protein bearing the point mutation was packaged into the virion as efficiently as the wild-type vhs protein. Like a mutant encoding truncated vhs, the RNase$^-$ virus showed IFN-dependent replication that was restricted compared with that of the wild-type virus. The RNase$^-$ virus was highly attenuated in wild-type mice infected intravaginally, with reduced mucosal replication, disease severity, and spread to the nervous system comparable to those of the vhs truncation mutant. Surprisingly, in alpha/beta interferon (IFN-α/β) receptor knockout mice, the vhs RNase mutant was more attenuated than the vhs truncation mutant in terms of disease severity and virus titer in vaginal swabs and central nervous system samples, suggesting that non-enzymatically active vhs protein interferes with efficient virus replication. Our results indicate that vhs enzymatic activity plays a complex role in vhs-mediated type I IFN resistance during HSV-2 infection.**

Herpes simplex virus 2 (HSV-2) is the primary etiologic agent of genital herpes, one of the most highly prevalent sexually transmitted infections in the Unites States and throughout the world (64, 52). HSV-2 undertakes both lytic and latent infection of its natural host. Primary lytic infection with HSV-2 begins in mucosal epithelial cells, with subsequent invasion of the innervating sensory neurons. By evading host defenses, HSV establishes life-long latency in the neuronal cell bodies of the host, from which occasional reactivation results in reinfection of the epithelia or mucosa. These mucosal lesions can be a source of viruses that are transmissible to new hosts.

Numerous HSV proteins, while nonessential, participate in the process of replication and spread to ensure successful infection. The virion host shutoff (vhs) protein has been identified as one such viral component. vhs has endonuclease activity specific for mRNA (9, 10, 61, 65). It degrades host and viral mRNAs (27, 28, 44, 46) and disrupts preexisting polyribosomes (17, 60), resulting in the rapid shutoff of host protein synthesis in the infected cell. As a tegument component, vhs is immediately delivered into the cytoplasm and is able to influence the cellular environment by modulating viral and cellular protein syntheses. The vhs protein itself functions as an RNase in vitro (61), but the interacting cellular translation initiation factors eIF4A, eIF4B, and eIF4H stimulate vhs activity and may be required to target its activity to mRNAs in vivo (7, 12, 15, 16, 34).

vhs proteins may perform other nonenzymatic functions as well. Because vhs is packaged into the virion, it may participate in tegument assembly by maintaining the optimal stoichiometry of tegument components. In addition, vhs interacts with VP16 (51) in a complex that includes VP22 (62) and may influence the subcellular localization and activities of its binding partners. vhs clearly contributes to HSV virulence in the host, as HSV-1 and HSV-2 vhs deletion mutants are highly attenuated in mouse models of ocular and genital infections, respectively (53, 54, 57). vhs mutants show restricted replication in vivo and have significantly reduced capacities to cause disease, establish latency, and reactivate. HSV-1 vhs also delays apoptosis of cultured infected neurons (2). What role each of these vhs functions may play in promoting HSV virulence is not known.

To achieve efficient replication and spread within the host organism, HSV must inhibit host antiviral defenses at the site of entry and in the tissues subsequently invaded. Numerous HSV proteins block host innate and acquired immune functions to ensure successful infection. Type I interferons (alpha/beta interferon [IFN-α/β]) potently inhibit viral replication in cells by stimulating the synthesis of a variety of antiviral effector molecules that can inhibit cellular macromolecular synthesis and induce apoptosis (1, 19). IFN-α/β also activates cellular host immune defenses such as NK cells, B lymphocytes, and cytotoxic T lymphocytes (19, 21). Thus, a virus's capacity to

* Corresponding author. Mailing address: Department of Molecular Microbiology and Immunology, Saint Louis University School of Medicine, 1100 S. Grand Blvd., St. Louis, Missouri 63104. Phone: (314) 977-8874. Fax: (314) 977-8717. E-mail: morrisla@slu.edu.

▽ Published ahead of print on 30 January 2008.

disarm the host type I IFN response cripples both innate and adaptive immune impediments to infection. Although IFN-α/β inhibits virus replication in the periphery and limits progression of HSV infection into the central nervous system (CNS) (20), HSV-1 and HSV-2 have evolved many specific means to counter the effects of IFN-α/β (30, 37), including roles for HSV-1 ICP34.5, Us11, and ICP0 (4, 5, 6, 22, 38, 39). Attenuated ICP0$^{-/-}$ and −ICP34.5$^{-/-}$ HSV-1 mutants regain wild-type levels of replication and virulence, respectively, in IFN-α/βR$^{-/-}$ mice (31, 32), attesting to their capacity to thwart the innate immune response to infection.

vhs has also been identified as an IFN-α/β resistance factor. Genetic mapping of HSV-1 IFN resistance identified a region that includes the vhs locus (58). HSV-1 vhs deletion mutants show little or no increased sensitivity to type I IFN in vitro (38, 59), and their replication in vivo is not significantly affected by IFN-α/β (31). In contrast, we have shown that the major attenuating factor for vhs-deficient HSV-2 in vitro and in vivo is the type I IFN response (8, 42), suggesting quantitative or qualitative differences in the capacity of HSV-1 and HSV-2 vhs proteins to modulate this branch of innate immunity. It seems logical that vhs may counter the IFN response by utilizing its ribonucleolytic activity to reduce IFN or IFN-stimulated gene expression, but the contribution of vhs ribonucleolytic activity to the overall effects of vhs on HSV-2 pathogenesis has not been examined.

One means to determine the role of vhs RNase activity in virulence without disruption of other vhs functions is selective abrogation of the enzymatic activity. vhs shares sequence homology with the FEN-1 family of ribonucleases (12), and the conserved amino acids essential for vhs RNase activity in HSV-1 vhs have been thoroughly mapped (12, 13). Therefore, we generated a HSV-2 strain containing a point mutation in vhs which abrogates vhs RNase activity but permits the synthesis of full-length vhs protein capable of fulfilling other potential vhs functions in the virus life cycle. We compared the vhs RNase-deficient virus with vhs deletion mutant and wild-type viruses in a mouse model of HSV-2 genital infection in terms of virulence and the capacity to counteract the host type I IFN response.

## MATERIALS AND METHODS

**Cells and viruses.** Vero cells were maintained in Dulbecco's modified Eagle's medium (DMEM) supplemented with 3% newborn calf and 3% bovine growth sera and 1% each of L-glutamine and penicillin-streptomycin (Invitrogen). Murine embryonic fibroblasts (MEFs) were generated from embryos at 16 to 17 days of gestation. The cells were cultured in DMEM supplemented with 10% bovine growth serum and were used through passage 3. HSV-2 strain 333d41 (54) has a targeted deletion in the UL41 gene between two XcmI sites, resulting in a 939-bp excision and complete lack of vhs activity. Wild-type HSV-2 strain 333 and the vhs deletion mutant 333-*vhs*B were generously provided by Jim Smiley. 333-*vhs*B (51) contains a cassette consisting of the ICP6 promoter driving the *lac*Z gene, inserted using the BstXI restriction site at codon 30 of the *vhs* open reading frame (ORF), thus disrupting the UL41 gene. Cell lysate and cell supernatant stocks of virus were prepared as previously described (35). The titers of the virus stocks were determined by titration on Vero cell monolayers (45).

**Isolation of mutant and rescue viruses.** Plasmid pvhs96M, obtained from David Leib (54), was constructed by ligation into the pGEM3Z vector (Promega) of a BamHI-FspI restriction fragment of HSV-2 333 containing the UL41 ORF flanked by portions of UL40 and UL42. The pvhsD215N plasmid was generated by site-directed mutagenesis of pvhs96M, using the Gene Tailor site-directed mutagenesis system (Invitrogen). The forward primer mutated a guanine to adenine at nucleotide 643 in the *vhs* ORF, causing the D215N amino acid substitution, and a silent cytosine to adenine change at nucleotide 648 to create a unique BglII site. Introduction of the nucleotide substitutions into pvhs96M were verified by restriction digestion and sequencing. To generate point mutant viruses, the pvhsD215N plasmid was linearized and cotransfected with full-length 333-*vhs*B DNA in the presence of Lipofectamine and Plus reagent (Invitrogen) according to the manufacturer's instructions. White plaques were isolated from the cotransfection culture, using standard X-Gal (5-bromo-4-chloro-3-indolyl-β-D-galactopyranoside; Invitrogen) staining procedures. The isolates were triply plaque purified and analyzed by PCR, restriction digestion, sequencing, and Southern blotting. One of the isolates, named D215N, was used to carry out all the experiments. Full-length DNA from the D215N virus was isolated and cotransfected with pvhs96M into Vero cells using an Amaxa Nucleofector kit according to the manufacturer's protocol (Amaxa Biosystems) to generate a repair virus. The progeny were screened for loss of the BglII site by PCR and BglII restriction digestion. The repair virus, D215NR, was plaque purified three times, and its genotype was verified by sequencing and Southern blotting.

**Southern blot analysis.** In order to verify the presence of the point mutation in D215N and the reconstitution of the UL41 ORF in D215NR, viral DNAs were purified from mutant and rescue viruses, using standard phenol-chloroform extraction. Five hundred micrograms of each DNA sample was subjected to BamHI and BglII restriction digestion, and the fragments were separated on a 0.8% agarose gel. The DNA fragments were transferred to a Hybond nylon membrane (Amersham) by capillary diffusion and hybridized to a randomly primed $^{32}$P-labeled pvhs96M vector as a probe. Images were obtained on X-ray film by autoradiography.

**Western blot analysis.** Cell lysates were prepared by mock infecting or infecting Vero cells at a multiplicity of infection (MOI) of 5 with either the 333 (wild-type), 333d41 (vhs$^-$ deletion mutant), D215N (vhs point mutant), or D215NR (rescue) virus. The cells were harvested at 14 h postinfection and lysed in RIPA buffer (50 mM Tris-HCl [pH 8.0], 150 mM NaCl, 0.5% sodium deoxycholate, 0.1% sodium dodecyl sulfate [SDS], 1% NP-40) mixed with 2× Laemmli buffer, heated at 95°C for 5 min, and then subjected to SDS-polyacrylamide gel electrophoresis (SDS-PAGE). After electrophoresis, the proteins were transferred to polyvinylidene difluoride (PVDF) membranes, which were blocked in Tris-buffered saline-Tween 20 (TBST) containing 5% nonfat dry milk. Incubations were carried out in TBST, using the murine monoclonal anti-vhs antibody 4F10.6 (obtained from David Leib) or rabbit anti-S6 antibody (Cell Signaling Technology) for normalization. Anti-mouse horseradish peroxidase-conjugated antibody (Sigma) and anti-rabbit alkaline phosphatase-conjugated antibody (Promega) were used for detection. All primary and secondary antibody incubations were carried out in TBST. Bands were visualized using enhanced chemiluminescence Western blotting detection reagents (Amersham) and blue film (Midwest Scientific) or NBT/BCIP (Nitro Blue Tetrazolium/5-bromo-4-chloro-3-indolylphosphate; Promega) according to the manufacturers' instructions.

**Plasmids.** To create pcDNA-333VP16, the complete ORF of HSV-2 VP16 was amplified by PCR, using Platinum high fidelity *Taq* polymerase (Invitrogen) and forward primer 5′-TTGAGGATCCATGGACCTGTTGGTCGACG-3′ and reverse primer 5′-ATGAGAATTCCTACCCCCCAAAGTCGTCAATGCCC-3′, and was cloned into the BamHI and EcoRI sites in pcDNA3.1 (Invitrogen). For pcDNA-333vhs-HA, the HSV-2 *vhs* ORF was fused to the hemagglutinin (HA) tag by PCR, using forward primer 5′-ATCAGGATCCATGGGTCTGTTTGGC ATGATGAAGTTTGCC-3′ and reverse primer 5′-ATCAGAATTCTCAAGC GTAGTCCGGTACGTCGTATGGGTACTCGTCCCAGAATTTAGCCAGG-3′, and was cloned into the BamHI and EcoRI sites in pcDNA3.1. Plasmid pcDNA-D215N-HA was created by replacing an AscI-AgeI restriction fragment of the pcDNA-333vhs-HA construct with the corresponding fragment of the pvhsD215N plasmid.

**RNA isolation and quantitative real-time PCR.** Monolayer cultures of $1.5 \times 10^6$ to $1.8 \times 10^6$ Vero cells were mock infected or infected at an MOI of 10 in the presence of 10 μg/ml of actinomycin D (Act D). Cytoplasmic RNAs were harvested at 6 h postinfection, using an RNeasy minikit (Qiagen), including the on-column DNase digestion step. RNA purity and integrity were examined on RNA Nano lab chips (Agilent). Five hundred nanograms of each RNA sample was reverse transcribed, using anchored-oligo(dT)$_{18}$ primers and a Transcriptor first-strand cDNA synthesis kit (Roche) in a 20-μl volume according to the manufacturer's instructions. Real-time PCRs to detect GAPDH (glyceraldehyde-3-phosphate dehydrogenase) mRNA and 18S rRNA were performed on 0.1 μl of cDNA, using FastStart Sybr green master mix (Roche) and an ABI Prism 7500 real-time PCR system (Applied Biosystems). Reactions were performed in duplicate in 25-μl volumes. The sequences of the GAPDH primers used are 5′-GAACGGGAAGCTTGTCATCAATGG-3′ and 5′-TGTGGTCATGAGTC CTTCCACGAT-3′, which amplify a 343-bp product. The sequences of the 18S rRNA primers used are 5′-GTAACCCGTTGAACCCCATT-3′ and 5′-CCATC

CAATCGGTAGTAGCG-3′ (63), which amplify a 151-bp product. The PCR parameters were 10 min of FastStart *Taq* activation at 95°C, followed by 40 cycles at 95°C for 20 s and at 60°C for 1 min. Specificity was verified by melting curve analysis. The GAPDH signal was normalized to the 18S rRNA signal, using the $2^{-\Delta\Delta CT}$ method (33, 45). The GAPDH mRNA level in mock-infected Vero cells was set at 100%, and the GAPDH mRNA level remaining in virus-infected samples was calculated as a percentage of that of the mock-infected cells.

**Metabolic labeling.** Cells (129 MEF) in 12-well plates ($2.3 \times 10^5$ cells per well) were mock infected or infected at an MOI of 10 with wild-type, vhs deletion mutant, RNase-deficient mutant, and rescue viruses in the presence or absence of 10 μg/ml Act D. After 1 h, the unabsorbed virus was removed, the monolayers were washed extensively, and DMEM plus 2% fetal bovine serum was added. At 5.5 h postinfection, the medium was replaced with methionine- and cysteine-free medium (Sigma) for 30 min, and then medium supplemented with 50 μCi/ml $^{35}$S-labeled methionine and cysteine (EasyTag Express [$^{35}$S]methionine-cysteine protein-labeling mix; PerkinElmer Life Sciences) was added to each well for 2 h. Prior to harvesting, the monolayers were washed three times with phosphate-buffered saline (PBS) and then scraped from the wells and collected in ice-cold PBS supplemented with protease inhibitors. The cells were spun at $1{,}000 \times g$ for 10 min at 4°C, and then the pellet was resuspended in 60 μl of RIPA buffer containing protease inhibitors (Complete mini; Roche) and an equal amount of 2× Laemmli buffer. The eluted protein was subjected to SDS-PAGE, transferred to PVDF membranes, and exposed to autoradiography film and then to a phosphoscreen (Molecular Dynamics). Images were scanned on a phosphorimager (Storm 860; GE Healthcare) and analyzed using ImageQuant TL software (Amersham Biosciences Limited). All membranes were subsequently subjected to Western blot analysis.

**Coimmunoprecipitation.** Vero cells in 6-well plates were mock transfected or cotransfected with 1 μg each of a plasmid expressing HSV-2 VP22 [pcDNA-VP22(2)], VP16 (pcDNA-VP16), and *vhs* (pcDNA-333vhsHA or pcDNA-D215NHA), using Lipofectamine and Plus reagent (Invitrogen) according to the manufacturer's instructions. After 48 h, the cells were lysed in 490 μl of immunoprecipitation (IP) buffer (50 mM Tris-HCL [pH 7.2], 150 mM NaCl, 1% Triton X-100) supplemented with protease inhibitor (Complete mini; Roche Diagnostics). The lysates were incubated on ice for 30 min, clarified at $17{,}000 \times g$ at 4°C for 10 min, and then precleared twice by incubation with protein A/G-agarose beads (Calbiochem). IP reactions were then carried out by mixing 200 μl of cell lysate with 20 μl of protein A/G-agarose beads bound to 1 μg of mouse anti-VP16 monoclonal antibody 1-21 (Santa Cruz) or 10 μl of mouse anti-VP22 monoclonal antibody 22-3 (18). As a control for a specific interaction, the lysates were incubated with bovine serum albumin-coated empty beads. The immunoprecipitates were mixed overnight at 4°C. The beads were pelleted and washed four times with ice-cold IP buffer, resuspended in 60 μl of 2× Laemmli buffer, and boiled for 5 min. Samples of the original lysate (8 μl) and IP samples (20-μl volumes, representing proteins immunoprecipitated from 67 μl of the original lysate) were subjected to 10% SDS-PAGE and analyzed by Western blotting, using 1-21, 22-3, or rat monoclonal anti-HA antibody 3F-10 (Roche). Anti-mouse and anti-rat alkaline phosphatase-conjugated secondary antibodies (Promega) were used for detection. Bands were visualized by using Nitro Blue Tetrazolium/BCIP (Promega) according to the manufacturer's instructions. In other experiments, Vero cells ($4 \times 10^6$ cells) in 100-mm dishes were mock infected or infected at a MOI of 10 with 333, D215NR, D215N, or 333d41, and lysates were prepared at 18 h postinfection for IP, as described above. For Western blotting for vhs, the murine monoclonal anti-vhs antibody 4F10.6 was used. Densitometric analyses were performed using ImageQuant software (Amersham Biosciences).

**In vitro growth curves.** Cells were seeded into 12-well plates 1 day prior to infection. Vero cell monolayers ($2.8 \times 10^5$ to $4.5 \times 10^5$ cells/well) were infected at a MOI of 10 (high MOI) or 0.01 (low MOI) with wild-type, vhs deletion mutant, RNase point mutant, and rescue viruses. The monolayers were collected by scraping at 8, 12, 16, 24, and 30 h (high MOI) or 8, 12, 16, 24, and 36 h (low MOI) and stored at −80°C. MEF monolayers ($2.5 \times 10^5$ cells/well) were infected at a MOI of 0.01. The cells were collected at 6, 24, 48, and 68 h and stored at −80°C. Samples were thawed and sonicated, and the titers were quantified by standard plaque assay on Vero cell monolayers (53).

**Animal studies.** IFN-α/βR$^{-/-}$ mice (41) and congenic 129 [129Sv(ev)] mice were generously provided by Michel Aguet and were obtained from Skip Virgin. The mice (129 wild-type and IFN-α/βR$^{-/-}$) were bred and housed in the Department of Comparative Medicine, Saint Louis University School of Medicine. All mice were maintained in accordance with institutional and PHS guidelines and were used at 6 weeks of age. The mice were infected intravaginally (i.vag.) with $1 \times 10^6$ PFU/mouse as previously described (36). Vaginal vaults were swabbed twice (at each time point) at 9 h and on days 1 through 5 postinfection, using type 1 calcium alginate swabs (Puritan). The swabs were placed together into vials containing 1 ml of PBS and stored at −80°C. On days 2 through 6 postinfection, the severity of genital and neurologic disease was assessed independently by two persons, using the following scale: 0, no signs; 1, mild erythema and edema of the external genitalia; 2, moderate erythema and edema; 3, genital lesions; 4, bilateral hind limb paralysis; and 5, death (36). At 6 days postinfection, the mice were sacrificed, and the spinal cord, brainstem, and brain were dissected, placed in microfuge tubes containing PBS and 1-mm glass beads, and stored at −80°C. Thawed tissues were disrupted, using a MiniBeadbeater-8 (BioSpec Products). The viral titers in swab samples and tissues were determined by standard plaque assay (26). In other experiments, the infected mice were monitored daily for survival and sacrificed when moribund.

To study virus replicative capacity in the CNS, anesthetized mice were infected intracranially in the right cortex with $1 \times 10^4$ PFU/mouse, using a 30-gauge needle and a 0.3-ml syringe (Terumo). Brain tissue was dissected at 18, 36, or 72 h postinfection and homogenized for the determination of virus titers.

**Statistics.** The significance of the difference in viral titers between groups was determined by the Student *t* test. The Kruskal-Wallis test was used to determine the significance of the differences in disease scores between groups on individual days. The significance of the differences in the proportions of mice surviving on individual days was compared using the Fisher exact method.

## RESULTS

**Construction of point mutant and rescue viruses.** Previous studies utilizing *vhs* deletion mutants have elucidated the striking benefit of the vhs protein to HSV-2 pathogenesis in mice. To determine the specific contribution of vhs RNase activity to the pathogenic potential of HSV-2, we constructed a virus that encodes full-length vhs protein with a targeted mutation that eliminates its enzymatic activity. Three considerations were weighed in selecting the mutation site. Each was based on previous characterizations of the HSV-1 vhs polypeptide, which shares 86% amino acid identity with HSV-2 vhs (11). First, four highly conserved domains within the vhs proteins of alphaherpesviruses that are important for ribonucleolytic function (14, 25) have been identified (3). Second, numerous point mutations in conserved residues of the HSV-1 vhs protein that abrogate RNase activity but retain eIF4H and eIF4A binding activity have been identified (12, 15, 16). Third, HSV-1 vhs contains VP16 interaction (48) and PEST (David Leib, personal communication) sequences that we wished to preserve. We chose to mutate amino acid 215 of HSV-2 vhs in conserved domain III, because mutation of the analogous site in HSV-1 vhs, amino acid 213, abrogates RNase activity without compromising known protein-protein interactions.

Site-directed mutagenesis was performed to generate an aspartic acid-to-asparagine substitution at amino acid position 215 of the vhs protein expressed from pvhs96M (54), which contains the UL41 ORF of HSV-2 strain 333. The nucleotide changes also introduced a new BglII restriction site (Fig. 1A). The resulting plasmid, pvhsD215N, was cotransfected with full-length DNA from the 333-*vhs*B strain (51), which contains a *lacZ* insertion in the *vhs* ORF. The cotransfection was screened for white plaques in the presence of X-Gal, and isolates were triply plaque purified. The presence of the point mutation was ascertained by BglII digestion of PCR-amplified UL41 and was confirmed by sequencing of the UL41 locus. One of the isolates was named D215N. To ensure that any effect of the point mutation on RNase activity or virulence was due solely to the engineered mutation, we restored the wild-type allele by cotransfection of viral DNA from D215N and pvhs96M, resulting in virus D215NR. Southern blot analysis was used to verify the genotypes (Fig. 1B). Viral DNAs were

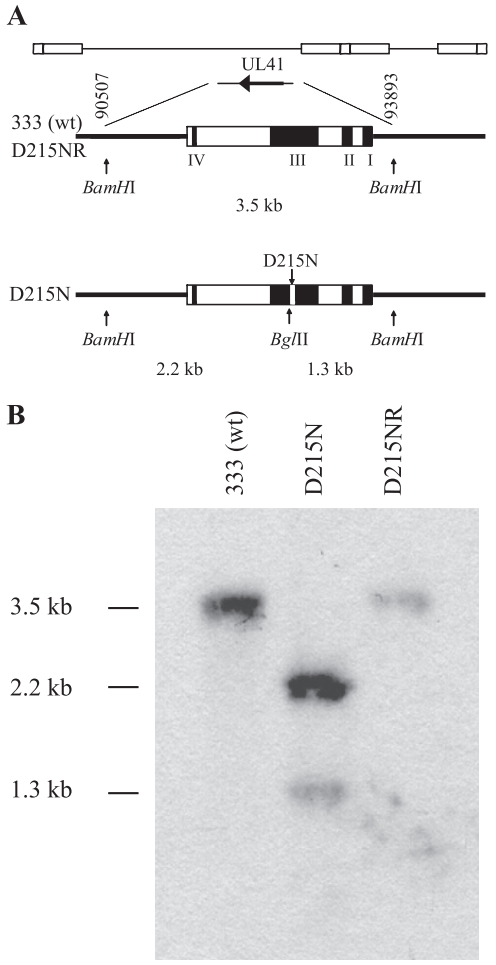


FIG. 1. Southern blot analysis of the *vhs* locus. (A) The genomic position of the UL41 ORF is shown on line 1. An expanded view of this region (line 2) depicts a 3.5-kb BamHI fragment that includes the wild-type (wt) *vhs* locus with its four domains that are important for RNase activity. Line 3 shows the location of the D215N mutation and the new BglII site. (B) Viral DNAs isolated from wild-type (333), vhs RNase-deficient (D215N), and RNase-deficient repair (D215NR) viruses were digested with BamHI and BglII, subjected to electrophoresis, and transferred to a membrane. The blot was probed with $^{32}$P-labeled pvhs96M DNA. The expected sizes of the fragments were 3,476 bp for the wild-type 333 and D215NR viruses and 2,145 bp and 1,331 bp for the D215N mutant.

restricted with BamHI and BglII, electrophoresed, transferred to membranes, and detected, using randomly primed pvhs96M as the probe. The Southern blot of the wild-type 333 and D215NR viruses showed a single fragment of the expected size (3.5 kb) (Fig. 1B, lanes 1 and 3), and that of D215N showed two fragments of the expected sizes (2.2 kb and 1.3 kb) (Fig. 1B, lane 2), consistent with the presence of a new BglII site introduced by the point mutation of UL41 in D215N that was restored in D215NR.

**vhs protein expression by the point mutant virus.** To demonstrate that the D215N point mutant virus expresses vhs protein in infected cells, Western blotting was performed on cell lysates collected 14 h postinfection. Membranes probed with a monoclonal antibody to vhs showed a band with mobility of approximately 58-kDa and equivalent intensity in the lysates of

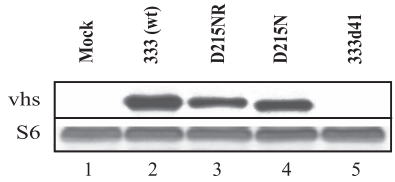


FIG. 2. Western blot analysis of vhs protein. Vero cells were mock infected or infected with the 333 (wild-type [wt]), D215NR (rescue), D215N, or 333d41 virus at a MOI of 5 and harvested 14 h postinfection. The proteins were separated by SDS-PAGE and transferred to a membrane. The blot was probed with an antibody to vhs (top) or ribosomal S6 (bottom) protein.

cells infected with HSV-2 333, D215NR, or D215N (Fig. 2, lanes 2 to 4) that was absent from mock- and 333d41-infected cells (Fig. 2, lanes 1 and 5). Reprobing with antibody to S6 ribosomal protein, which was used as a loading control because of its low turnover rate, showed that S6 levels were similar in all samples (Fig. 2); therefore, vhs protein is produced by the D215N mutant at approximately wild-type levels. vhs produced in cells infected with the D215N mutant had slightly increased mobility compared with the wild-type and rescue viruses. This altered mobility likely did not result from a difference in the phosphorylation state, because the relative mobilities of wild-type and mutant vhs did not change upon treatment with calf intestinal alkaline phosphatase (data not shown). Instead, the aspartic acid-to-asparagine change may have altered the charge and possibly the conformation of vhs, resulting in the slightly increased mobility.

**The D215N mutation ablates vhs RNase activity.** To verify the loss of RNase activity in vhs mutant viruses, Vero cells were mock infected or infected with 333 (wild-type), D215NR (rescue), D215N, or 333d41 (vhs deletion mutant) (54). At 6 h postinfection, cytoplasmic mRNA was isolated and polyadenylated mRNAs were reverse transcribed. The cDNAs were used as templates for the quantitative real-time PCR determination of GAPDH mRNA in samples normalized to the content of 18S rRNA. The GAPDH mRNA level in mock-infected cells was set at 100%, and the GAPDH mRNA level remaining in the virus-infected samples was calculated as a percentage of that of the mock-infected cells. Cells infected with the wild-type and rescue viruses contained only 10% of the GAPDH mRNA found in mock-infected cells (Fig. 3). In contrast, cells infected with the D215N point mutant and 333d41 deletion mutant viruses showed levels of GAPDH equivalent to that of mock-infected cells, indicating that the single-amino-acid change in HSV-2 vhs abrogated RNase activity.

We next determined the effect of the loss of RNase activity on global virion-induced host shutoff. Cells were infected with 10 PFU per cell of the various viruses in the presence or absence of Act D and labeled with [$^{35}$S]methionine-cysteine from 8 to 10 h postinfection, and the levels of host cell protein synthesis were determined (Fig. 4). The wild-type and rescue viruses showed a decrease in de novo protein synthesis compared with that of the mock-infected cells (Fig. 4A), which was even more apparent in the presence of Act D. The levels of the S6 ribosomal protein remained relatively constant (Fig. 4B). In contrast, both the D215N and 333d41 mutant viruses failed to induce generalized shutoff of protein synthesis in the infected

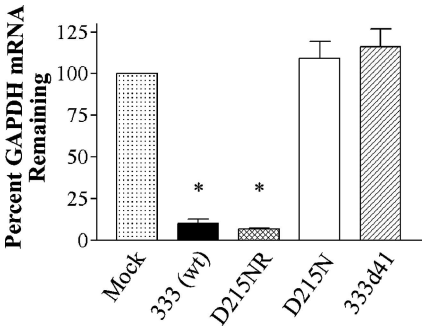


FIG. 3. Real-time PCR detection of RNase activity. Vero cells were mock infected or infected with the 333 wild type [333 (wt)], D215NR (rescue), D215N, or 333d41 virus at a MOI of 10 in the presence of Act D and harvested 6 h postinfection. Total cytoplasmic RNA was isolated from the samples and reverse transcribed to cDNAs. These cDNAs were used as templates for quantitative real-time PCR detection of GAPDH and 18S rRNA transcript levels in the original samples. Relative changes in the GAPDH transcript levels of the virus-infected samples compared to those for the mock-infected samples, all normalized for 18S rRNA expression, were determined, using the $2^{-\Delta\Delta CT}$ method. The GAPDH mRNA level remaining in the virus-infected samples was calculated as a percentage of that of the mock-infected samples. The data were compiled from two experiments, each performed in duplicate. *, $P < 0.0001$ for the results for the wild-type and D215NR virus-infected samples compared with that for the mock-infected samples.

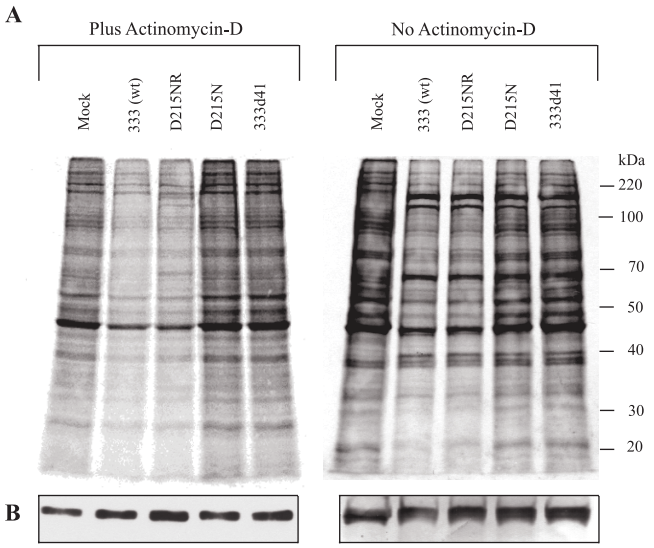


FIG. 4. Effect of wild-type and mutant HSV-2 on host protein synthesis in the absence and presence of Act D. 129 MEF cells were mock infected or infected with 10 PFU of 333 (wt), D215NR, D215N, or 333d41 per cell in the presence or absence of Act D and harvested at 10 h postinfection. (A) The cultures were pulse labeled with [$^{35}$S]methionine and [$^{35}$S]cysteine for the last 2 h before being harvested. Whole-cell lysates were prepared, and the labeled polypeptides were subjected to 10% SDS-PAGE and transferred onto PVDF membranes, scanned on a Phosphorimager, and analyzed using ImageQuant TL software. A scale of molecular weights is shown to the right of the second panel. (B) The same membranes were probed with anti-S6 antibody to demonstrate uniform loading. wt, wild type.

host cells, indicating that the D215N point mutation in HSV-2 vhs affects global host shutoff activity to the same extent as deletion of vhs.

**HSV-2 VP16 coimmunoprecipitates with wild-type vhs or D215N.** The interaction between vhs and VP16 in a complex that includes VP22 is well documented for HSV-1 (29, 50, 55, 62). We determined whether HSV-2 vhs forms a similar complex and whether it is maintained in the D215N mutant. Vero cells were mock transfected or transfected with plasmids expressing HSV-2 VP22, VP16, and vhs-HA or D215N-HA. Cell lysates were prepared 48 h after transfection and subjected to IP, followed by Western blotting for VP22, VP16, or vhs (Fig. 5). The lysates of triply transfected cells but not of mock-transfected cells contained VP16, VP22, and wild-type vhs-HA or D215N-HA (Fig. 5A and B, lanes 1 to 3). After IP with anti-VP22, VP16, vhs-HA, and VP22 were each detected by Western blotting (Fig. 5A, lane 5). Faint background bands similar to the mobility of VP22 were detected in the immunoprecipitates of mock-transfected cells probed for VP22 (Fig. 5A, lane 4), but VP22 was clearly detectable above this background in VP22-transfected cells (Fig. 5A, lanes 5 and 6). IP using empty beads incubated with the lysates of triply transfected cells did not yield any specific bands (Fig. 5A, lanes 7 and 8). Importantly, D215N-HA was detected in the complex immunoprecipitated with anti-VP22 as readily as that with vhs-HA (the ratios of immunoprecipitated protein to input protein = 0.86 and 0.95, respectively, by densitometry) (Fig. 5A, lanes 5 and 6). For further confirmation of HSV-2 vhs-VP16 complex formation, the lysates of triply transfected cells were subjected to IP with antibody to HSV-2 VP16 (Fig. 5A, lower panel). Western blotting for VP16, vhs-HA, or VP22 demonstrated the presence of the proteins in the lysates (Fig. 5A, lower panel, lanes 2 and 3) and VP16 in the immunoprecipitates (Fig. 5A, lower panel, lanes 5 to 6). VP22 could not be unambiguously detected after IP because of background bands in the IP samples (Fig. 5A, lower panel, lanes 4 to 6). As predicted from IP with anti-VP22, vhs-HA and D215N-HA were both detected by Western blotting in the immunoprecipitates, using anti-VP16 (Fig. 5A, lower panel, lanes 5 and 6). Densitometric analyses indicated that the ratio of immunoprecipitated to input protein was similar for each (0.35 for vhs-HA, 0.45 for D215N-HA).

To demonstrate that a tripartite interaction between VP16, vhs, and VP22 occurs in HSV-2 infection, cells were infected with wild-type or rescue virus or either RNase mutant virus. Lysates were prepared 18 h postinfection and immunoprecipitated with an antibody to VP22, followed by Western blotting for VP16, vhs, or VP22 (Fig. 5B). Mock-infected cells showed no specific bands (Fig. 5B, lane 1), whereas the immunoprecipitates from cells infected with 333, D215NR, or D215N contained VP16, vhs, and VP22 (Fig. 5B, lanes 2 to 4). In the immunoprecipitates of cells infected with 333d41, only VP16 and VP22 could be detected (Fig. 5B, lane 5), suggesting a direct interaction between these two proteins in HSV-2-infected cells that does not depend on the presence of vhs. The immunoprecipitates from IP reactions using empty beads contained none of the three viral proteins (Fig. 5B, lane 6), confirming the specificity of the interactions observed with anti-VP22. Taken together, these results demonstrate that, like HSV-1 vhs, HSV-2 vhs can be found during infection in tripartite complexes that contain VP16 and VP22. These tripartite complexes also probably exist in triply transfected cells,

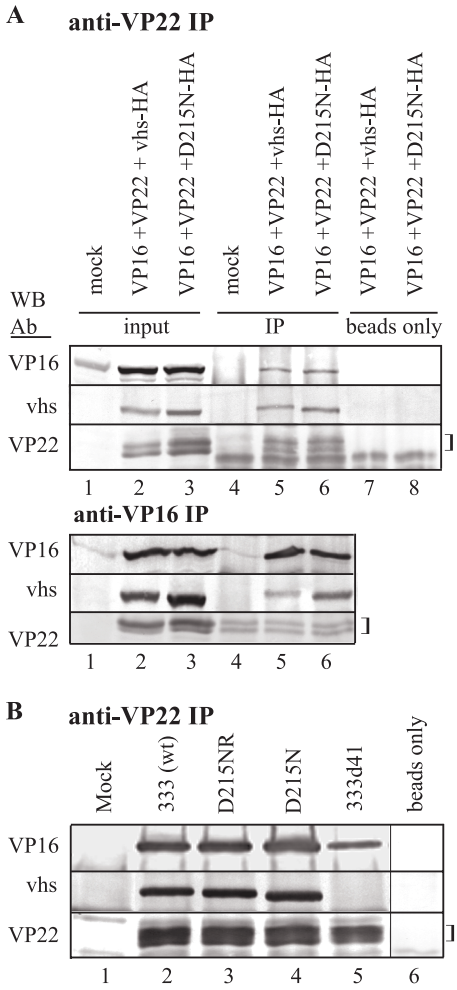


FIG. 5. Coimmunoprecipitation of HSV-2 vhs and VP16. (A) Vero cells were mock transfected or transfected alone or in combination with plasmids encoding HSV-2 VP22, VP16, vhs-HA, or D215N-HA. Lysates were prepared at 48 h posttransfection and subjected to immunoprecipitation with anti-VP22 or anti-VP16 coupled to protein A/G agarose beads. Proteins from the original lysates or that were eluted from the beads were separated by SDS-PAGE and transferred to membranes in duplicate. One divided membrane was probed by Western blotting with antibodies to vhs or VP22. The second membrane was probed for VP16. The experiment was repeated once with similar results. (B) Vero cells were mock infected or infected with the indicated virus. Lysates were prepared 18 h postinfection and subjected to IP with anti-VP22 coupled to protein A/G agarose beads or with beads alone. Proteins eluted from the beads were separated by SDS-PAGE and transferred to membranes and probed for vhs, VP22, or VP16, as described above. The experiment was repeated once with similar results. Brackets indicate background bands similar to the mobility of the VP22 isoforms. wt, wild type.

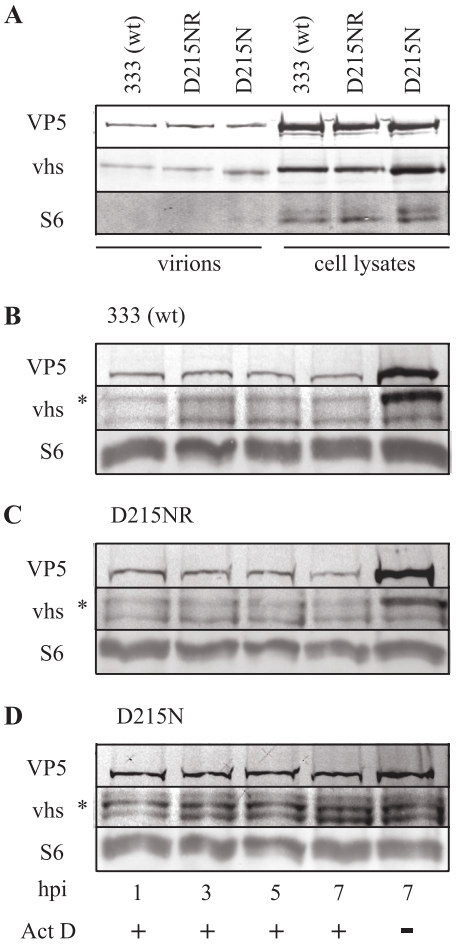


FIG. 6. Mutant vhs is packaged into virions and is stable in infected cells. Virions ($5 \times 10^5$ PFU) isolated from the supernatant of infected cells or equivalent PFUs of infected cell lysates were solubilized in Laemmli buffer, subjected to SDS-PAGE, and transferred to PVDF membranes. (A) Divided membranes were subjected to Western blotting, using antibodies to VP5, vhs, or S6. (B to D) Vero cells were infected at a MOI of 50 with the supernatant-derived virus 333 (B), D215NR (C), or D215N (D) in the presence or absence of Act D. The cells were lysed at the indicated times postinfection, and the proteins were separated by SDS-PAGE and transferred to membranes. Divided membranes were probed by Western blotting with antibodies to VP5, vhs, or S6. hpi, hours postinfection. wt, wild type.

although a reciprocal IP was unable to clearly demonstrate the presence of VP22. Most importantly, vhs bearing the D215N mutation also coimmunoprecipitated with VP16 and VP22, indicating that the loss of enzymatic activity does not affect the capacity of vhs to exist in a stable complex that contains VP16 and VP22.

**Mutant vhs protein is packaged into the virion and is stable in infected cells.** HSV virions contain approximately 200 copies of vhs (23, 47). The vhs protein may help maintain proper stoichiometry of tegument components during packaging and may participate in protein-protein interactions within the cell, such as binding to VP16 and cellular components of the translation machinery, eIF4A, eIF4B, and eIF4H. To determine whether vhs carrying the D215N mutation is packaged into the HSV particle, cell-free virions were isolated from infected culture supernatants. vhs protein and the capsid protein VP5 were readily detectable in equivalent amounts by Western blotting of $5 \times 10^5$ PFU of the supernatant-derived wild-type or D215N virus (Fig. 6A, lanes 1 and 3). Only a faint band was observed after Western blotting of supernatant-derived virions for the ribosomal protein S6 (Fig. 6A, lanes 1 to 3), but abundant S6 ribosomal proteins were observed in cell lysates containing $5 \times 10^5$ PFU of the viruses (Fig. 6A, lanes 4 to 6), indicating that cell-free virions are highly enriched in the supernatants of

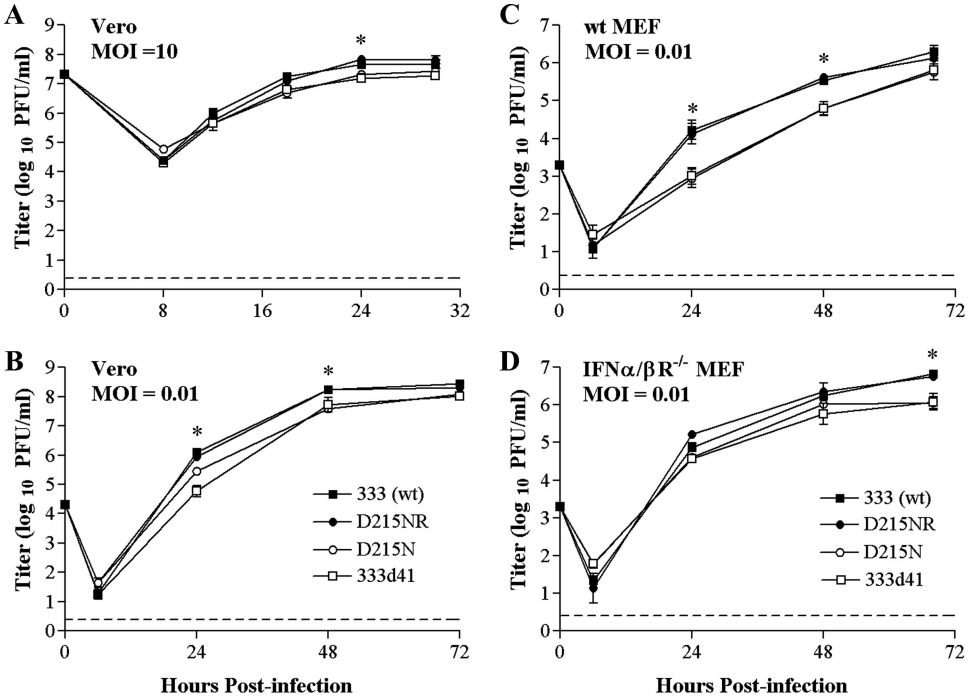


FIG. 7. Multistep growth in cultured cells. Replicate monolayers of Vero cells were infected with 333 (wt), D215NR, D215N, or 333d41 at a MOI of 10 (A) or 0.01 (B). Monolayers were collected at the indicated times, and viral titers were determined by standard plaque assay. MEFs (129, panel C, or IFN-$\alpha/\beta R^{-/-}$, panel D) were infected at a MOI of 0.01 with the viruses indicated above. Cultures were harvested at the indicated times, and viral titers were determined by plaque assays. The data points are the geometric means ± the standard errors of the means (SEM) of the results for duplicate wells from three independent experiments. The dashed line indicates the limit of detection. *, $0.0091 < P < 0.029$ (for the results for 333d41 and D215N compared with that for 333). wt, wild type.

infected culture supernatants. Because vhs protein bearing the D215N mutation is packaged into the virion, we next determined its stability relative to that of wild-type vhs in the newly infected cell. Supernatant-derived virus was used to infect Vero cells at a MOI of 50 in the presence or absence of Act D, and Western blotting was performed on cell lysates collected at various times postinfection. S6 was used as a control to ensure equal loading. vhs protein was detectable at 1 h postinfection in cells infected with the 333, D215NR, and D215N viruses (Fig. 6B to D, lane 1). This input vhs protein remained stable in both wild-type and mutant virus-infected cells through 7 h postinfection (Fig. 6B to D, lanes 2 to 4). The lower band on the vhs blot is a cross-reacting cellular protein. Cells infected with the 333 or D215NR virus for 7 h in the absence of Act D contained substantially more VP5 and vhs protein than was found in Act D-treated cells (Fig. 6B to D, lane 5). Interestingly, vhs and VP5 accumulated to a lesser extent in cells infected with D215N, suggesting the delayed onset of viral protein synthesis or less-vigorous protein synthesis in cells infected with the RNase-deficient virus. These results indicate that the mutant vhs protein is packaged into virions as efficiently as wild-type protein and that the virion-derived mutant vhs protein is as stable over time in infected cells as the wild-type protein.

**Multistep growth in cultured cells.** The vhs-deficient mutant 333d41 replicates nearly as well as wild-type HSV-2 in Vero cell cultures infected at high or low MOIs but is impaired for growth after infection of primary MEFs at a low MOI due to the effects of IFN-$\alpha/\beta$ (8). To ascertain whether the growth kinetics and IFN sensitivity of an RNase-deficient virus are similar to those of a vhs-deficient virus, we compared the replication of D215N and 333d41 with those of the 333 and D215NR viruses after infection of Vero and MEF cultures at high or low MOIs. In Vero cells infected at a high MOI (10), all the viruses grew similarly (Fig. 7A), and after infection of Vero cells at a low MOI (0.01), the growth of D215N and 333d41 lagged only slightly behind that of the wild-type and rescue viruses 333 and D215NR until late times postinfection (Fig. 7B). In primary 129 MEF cells infected at a low (0.01) MOI, both vhs mutant viruses grew significantly more slowly than 333 and D215NR, replicating to 1.5-log-lower titers at 24 h postinfection. This difference gradually decreased over time (Fig. 7C). In contrast to their replication in wild-type 129 MEF cultures, all the viruses replicated to similar titers in IFN-$\alpha/\beta R^{-/-}$ MEF cultures infected at a low MOI (Fig. 7D) until late times postinfection, when the titers of 333 and D215NR diverged from those of D215N and 333d41 ($P < 0.029$ for 333d41 and D215N compared with the titers for 333). In all cell types, D215NR replicated to the same levels as the wild-type virus, indicating successful restoration of the vhs allele. Thus, no significant differences exist in the growth characteristics of RNase-deficient and vhs-deficient viruses in vitro. In addition, restoration of D215N and 333d41 growth in IFN-$\alpha/\beta R^{-/-}$ MEFs suggests the involvement of RNase activity in countering the antiviral effects of IFN-$\alpha/\beta$.

**In vivo growth and virulence.** vhs-deficient mutants of HSV-2 are highly attenuated in vivo (42, 54). However, replication and especially virulence of vhs-deficient HSV-2 are

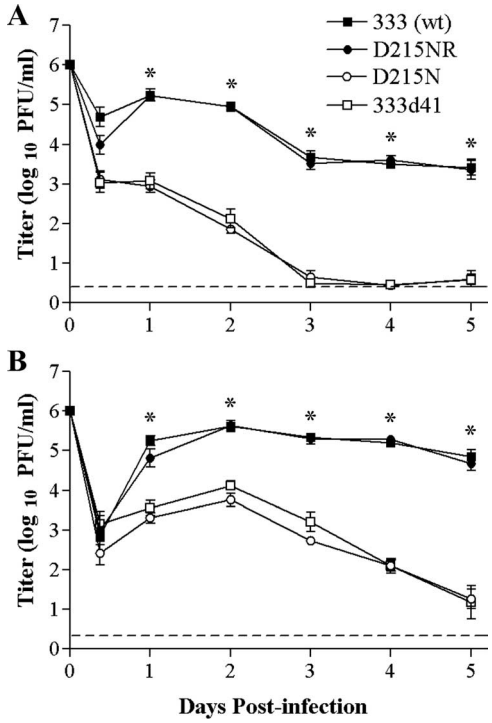


FIG. 8. Viral replication in the genital mucosa of 129 and IFN-α/βR$^{-/-}$ mice. Groups of mice were infected i.vag. with $1 \times 10^6$ PFU of the indicated virus strains. The titers of virus in vaginal swab samples of 129 mice ($n$ = 6 to 7) (A) and IFN-α/βR$^{-/-}$ mice ($n$ = 6) (B) were determined by standard plaque assays. The data points represent the geometric means ± SEM of the results for all samples per group. The dashed line indicates the limit of detection. *, $P < 0.0001$ for the results for the 333d41 and D215N mutant viruses compared with that for 333 (wt). The experiment was repeated once with similar results. wt, wild type.

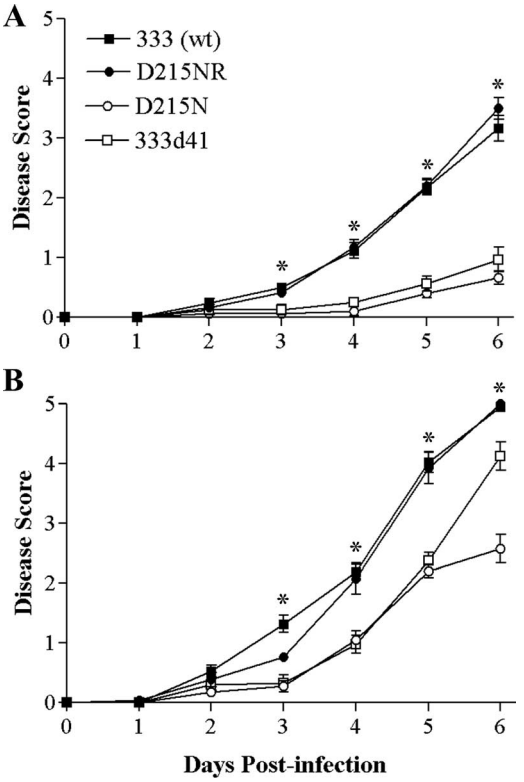


FIG. 9. Severity of genital and neurological disease in 129 and IFN-α/βR$^{-/-}$ mice. Mice (as described in the legend to Fig. 8) were scored for signs of disease. The values for 129 mice ($n$ = 15 to 25) (A) and IFN-α/βR$^{-/-}$ mice ($n$ = 13 to 20) (B) represent the arithmetic means ± SEM. *, $P \leq 0.001$ for the results for the D215N or 333d41 mutant viruses compared with that for the 333 (wt). The data were compiled from two independent experiments. wt, wild type.

markedly increased in IFN-α/βR$^{-/-}$ mice compared with those of wild-type mice (42), indicating that vhs plays an essential role in counteracting the type I IFN response to promote HSV-2 pathogenicity. We investigated whether the RNase activity of vhs is the critical determinant of the vhs protein's contribution to HSV-2 virulence.

IFN-α/βR$^{-/-}$ and congenic 129 mice were infected i.vag. with $1 \times 10^6$ PFU of 333, 333d41, D215N, or its rescuant, D215NR, and replication and virulence were monitored over time. In wild-type 129 mice, D215N and 333d41 replicated similarly in the genital mucosa but at least 100-fold less efficiently than 333 and D215NR on the first day postinfection. At all subsequent time points, the mutant viruses replicated to approximately 1,000-fold-lower titers than the wild type, reaching the limit of detection by day 3 postinfection (Fig. 8A). In IFN-α/βR$^{-/-}$ mice, both vhs mutant viruses recovered some capacity to replicate relative to that of the wild-type and rescue viruses over the first 2 days postinfection (Fig. 8B) and maintained higher titers on days 3 through 5 compared with their levels of replication in 129 mice. There was no significant difference in replication levels between 333 and D215NR in either host, indicating that the rescue virus indeed restored the wild-type phenotype. Interestingly, in IFN-α/βR$^{-/-}$ mice, D215N was slightly more attenuated than 333d41 over the first 3 days postinfection, although the difference did not achieve statistical significance.

Signs of genital disease in wild-type 129 mice infected with 333 and D215NR became apparent by the third day postinfection (Fig. 9A), with hind limb paralysis developing by 6 days postinfection. In contrast, infection with either D215N or 333d41 resulted in mild genital inflammation and no genital lesions or neurological signs. In IFN-α/βR$^{-/-}$ mice, the wild-type and rescue viruses showed a similar course of disease, but it was accelerated by approximately 1 day compared with that in 129 mice (Fig. 9B). Both vhs mutant viruses possessed a more virulent phenotype in IFN-α/βR$^{-/-}$ mice, with their course of disease accelerated by approximately 2 days compared with that of 129 mice. 333d41 approached the wild-type virus in virulence by 6 days postinfection, but interestingly, at that point the virulence of 333d41 and D215N diverged significantly ($P < 0.001$). Fully 40% of the mice infected with 333d41 were paralyzed by 6 days postinfection, while hind limb paralysis had occurred by day 6 postinfection in only 10% of the mice infected with D215N. These data indicate that the RNase activity of vhs plays an important role in vhs-dependent virulence and suggest a particular role in the neurovirulence of HSV-2.

To assess virus spread to and replication in the nervous system, some mice were sacrificed 6 days postinfection, and

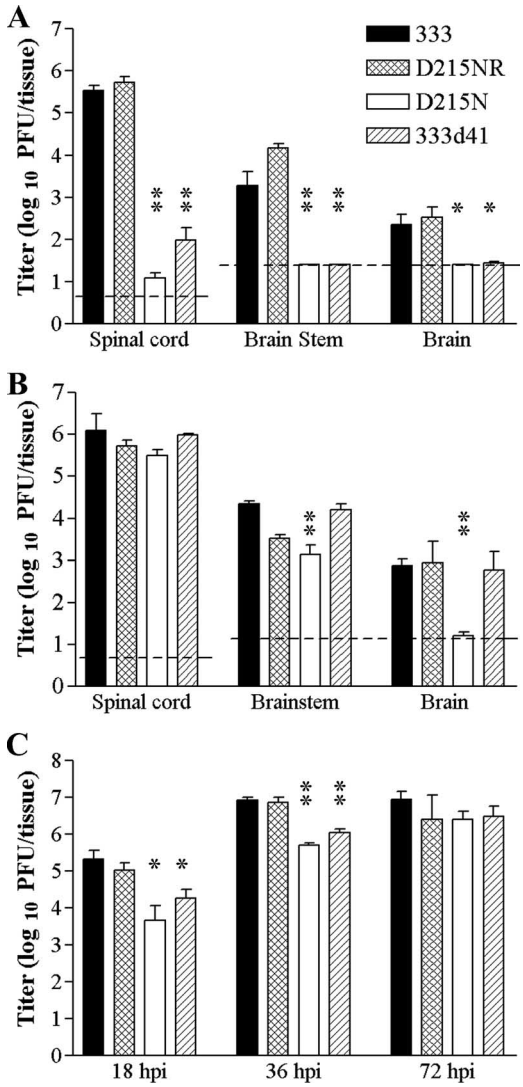


FIG. 10. Virus replication in the CNS. Groups of mice as described in the legend to Fig. 8 were sacrificed on day 6 postinfection. Brain, brainstem, and spinal cord tissues of 129 ($n$ = 6 to 10) (A) and IFN-α/βR$^{-/-}$ ($n$ = 6 to 11) (B) mice were disrupted by bead beating, and viral titers were determined by standard plaque assays. The dashed line indicates the limit of detection. (C) Groups of IFN-α/βR$^{-/-}$ mice ($n$ = 4 to 6) were infected intracranially with $1 \times 10^4$ PFU of the indicated viruses and sacrificed 18, 36, or 72 h postinfection. The viral titers in the brain were determined as described above. **, $P < 0.0001$ to $P = 0.0006$; *, $P = 0.0074$ to 0.0139 for the results for D215N compared with that for 333 (wild type). The data were compiled from two independent experiments.

their brains, brainstems, and spinal cord tissues were collected. The titers of D215N and 333d41 in the spinal cords of 129 mice were much lower than those of 333 and D215NR (Fig. 10A) and could not be detected in the brainstems and the brains. In contrast, in IFN-α/βR$^{-/-}$ mice, 333d41 replicated to levels equivalent to that of 333 and D215NR in all portions of the CNS (Fig. 10B), signifying the role of HSV-2 vhs in counteracting the type I IFN response. However, the titers of D215N in the spinal cords of IFN-α/βR$^{-/-}$ mice were still depressed relative to those of 333d41 ($P = 0.0039$), remained low in the brainstems ($P < 0.0001$ compared with the titers for 333d41), and were nearly undetectable in the brains ($P < 0.0001$ compared with the titers for 333d41) (Fig. 10B). Thus, the RNase activity-deficient mutant did not achieve the same degree of recovery in growth in the nervous systems of IFN-α/βR$^{-/-}$ mice as did the vhs-deficient mutant 333d41. To distinguish whether the persistent attenuation of D215N represented reduced capacity to spread to the nervous system or reduced capacity to replicate in neural tissues, IFN-α/βR$^{-/-}$ mice were infected intracranially with the wild-type, rescue, or mutant virus. Brain tissue was collected at several times postinfection, and virus titers were determined. At 18 and 36 h postinfection, replication of 333d41 and D215N in brain tissue lagged significantly behind that of 333 and D215NR (Fig. 10C), and even when directly inoculated into the nervous system, D215N replicated slightly less well than 333d41 ($P = 0.0199$ at 36 h for D215N compared with that for 333d41). By 3 days postinfection, the titers were roughly equivalent among all the viruses (Fig. 10C). This result indicates that the mutation abolishing vhs RNase activity impaired virus replication in the CNS but that both vhs mutant viruses were eventually able to achieve the same endpoint titers as the wild-type virus.

Intravaginal infection of mice with wild-type HSV-2 causes a severe and rapidly lethal infection, but viruses lacking vhs are attenuated (54). To examine the eventual outcome of infection with D215N, we determined the survival rate of mice infected with the wild-type or vhs mutant viruses. As expected, 129 mice infected with 333 and D215NR showed a steep decline in survival between days 6 and 7 postinfection (Fig. 11A). Notably, wild-type 129 mice infected with either D215N or 333d41 exhibited a more-gradual decline in health, and no genital lesions or hind limb paralysis was observed even at later times postinfection (Fig. 11A). However, all wild-type mice infected with the vhs mutant viruses eventually succumbed. In IFN-α/βR$^{-/-}$ mice, a steep decline in survival occurred between days 5 and 6 in those infected with 333 or D215NR (Fig. 11B). All mice infected with 333d41 also succumbed by 7 days postinfection, while the survival rate of mice infected with D215N exhibited a more-gradual decline through 9 days postinfection. Thus, infection with the RNase activity-deficient virus progresses more slowly to a lethal level than that with the vhs deletion virus in IFN-α/βR$^{-/-}$ mice, but all the viruses ultimately caused lethal infections in both wild-type and IFN-α/βR$^{-/-}$ mice.

## DISCUSSION

Using a vhs deletion mutant virus, we had previously demonstrated that HSV-2 vhs plays a prominent role in counteracting the host type I IFN response. The specific contribution of vhs RNase activity to the pathogenesis of HSV-2 could not be adequately addressed with a vhs deletion virus, however, because of the probable roles of vhs in virion structure as well as in complex formations with viral and cellular proteins. A mutant virus in which the enzymatic activity of vhs was selectively abrogated by point mutation was thus created. The point mutant virus, D215N, encodes a full-length vhs protein devoid of RNase activity that is efficiently incorporated into virions and retains the capacity to bind VP16 and to form complexes that include VP22, thus satisfying the requirement for an as-

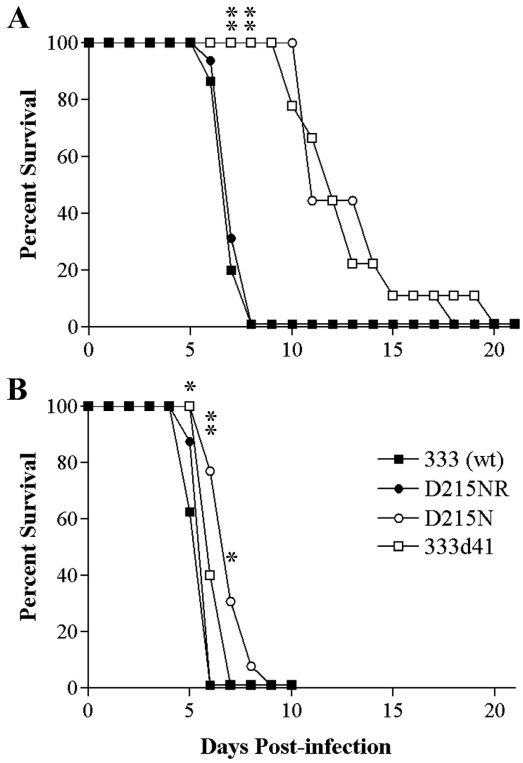


FIG. 11. Survival of mice after intravaginal infection. Groups of 6-week-old 129 ($n$ = 15 to 16) (A) and IFN-$\alpha\beta R^{-/-}$ ($n$ = 8 to 13) (B) mice were infected as described in the legend to Fig. 8, and their survival was monitored daily. **, $P \leq 0.0001$; *, $P = 0.0191$ to 0.0471 for the results for 333d41 and D215N compared with that for 333 (wt). wt, wild type.

sessment of RNase activity in an otherwise-intact virus. Multistep growth analysis using MEFs showed an initial growth delay of the vhs point mutant virus, with later recovery of growth to the level of the wild-type virus. The growth delay is related to an inability to counteract the type I IFN response; growth recovery was seen on IFN-$\alpha/\beta R^{-/-}$ MEFs. In wild-type mice, the RNase-deficient mutant D215N was attenuated for replication in the genital tract and for spread to the nervous system and recovered some capacity to replicate and cause disease in IFN-$\alpha/\beta R^{-/-}$ mice, indicating that RNase activity is crucial to the capacity of vhs to counteract the type I IFN response. Surprisingly, D215N remained more attenuated than a vhs null mutant virus in IFN-$\alpha/\beta R^{-/-}$ mice, suggesting the possibility of supplementary negative effects of the enzymatically inactive vhs protein.

vhs is a multifunctional protein. In addition to RNase activity, HSV-1 vhs interacts with VP16 through a 21-amino-acid-long region (48). The VP16-interacting domain of HSV-1 vhs is conserved in 15 of 21 amino acid residues with the analogous region of HSV-2 vhs, although it cannot be assumed that the residues through which intermolecular contacts occur are conserved. Interaction of VP16 with vhs is thought to attenuate vhs RNase activity, permitting late events in replication such as $\gamma 2$ protein expression to proceed. Recently, a tripartite interaction between HSV-1 VP16, vhs, and VP22 was demonstrated to be the critical attenuating unit (62). Attenuation of vhs activity via this complex appears to be essential for HSV viability, because VP22-deficient viruses also bear mutations in the *vhs* gene that result in defective vhs activity (49). We now present evidence that a complex containing HSV-2 vhs, VP16, and VP22 also forms, as these could be coimmunoprecipitated from triply transfected cells using an antibody to VP22 and from infected cells. Importantly, complex formation is maintained with D215N, indicating that the point mutation did not disrupt these interactions. In addition to VP16 and VP22, vhs forms a complex with cellular translation initiation factors eIF4A, eIF4B, and eIF4H (7, 15, 16). We selected the mutation site within HSV-2 vhs based on mutations within HSV-1 vhs that preserve interactions with eIF4A and eIF4H (15), but formal demonstration of HSV-2 vhs complex formation with these translation initiation factors remains to be carried out. Packaging of the tegument into the virion with proper stoichiometry is a second probable function of the interaction between vhs and other tegument components. We found vhs protein bearing the D215N mutation to be efficiently packaged into virions, thus preserving its likely structural role in tegument formation. Efficient packaging of the enzymatically inactive vhs protein into the tegument was expected, because tegument incorporation requires the amino terminal 42 amino acids of vhs (40), which are far removed from the D215N mutation.

The greatest challenge to a mutant virus is the test of in vivo fitness. We had anticipated that specifically abrogating the RNase activity of vhs would attenuate HSV-2 but not as profoundly as complete deletion of vhs because of the other known and potential functions of the vhs protein. In wild-type mice, both 333d41 and D215N were equally attenuated for replication in the genital mucosa. In survival assays performed with wild-type mice, infections with either the RNase or truncated vhs mutants resulted in delayed mortality compared with the kinetics of wild-type and rescue virus infection. These observations reinforce the notion that in wild-type mice, the RNase function of vhs is the most important contributor to vhs-mediated pathogenesis. Interestingly, although the RNase mutant and deletion mutant viruses could barely be detected in the nervous systems of wild-type mice by 6 days postinfection, they eventually caused lethal infections with similar kinetics. Thus, infection with RNase mutant viruses progresses more slowly to lethal infection than that with the wild-type virus, but all the viruses ultimately caused lethal infections in wild-type mice. Whether the lethality of the vhs mutants is a function of delayed neuronal infection or damage to other organs is not known.

We had previously shown that type I IFNs are a major attenuating factor for HSV-2 lacking vhs (8, 42). As with 333d41, D215N shows some recovery of replication in the genital mucosa of IFN-$\alpha/\beta R^{-/-}$ mice. Slight differences in replication in the genital tract between D215N and 333d41 were not statistically significant. From these data and the equivalent attenuation of D215N and 333d41 in wild-type mice, it is tempting to conclude that all the effects of vhs on pathogenesis are related to RNase activity, but in fact, analyses of virus replication in the nervous systems of IFN-$\alpha/\beta R^{-/-}$ mice revealed that enzymatically inactive vhs may have additional deleterious effects on the fitness of the point mutant virus. In IFN-$\alpha/\beta R^{-/-}$ mice, D215N proved even more atten-

uated than 333d41 in its capacity to cause paralysis by 6 days postinfection. This attenuated disease phenotype correlated well with the lower viral titers of the RNase mutant in the CNS compared with that of the deletion mutant at the same time point. The differences appear cumulative: a slightly lower level of replication of D215N in the genital tract apparently leads at each step to further attenuation, with reduced inflammation and delayed development of lesions and paralysis. These results suggest that the non-enzymatically active vhs protein may interfere with efficient virus replication and spread within the host, although the survival time is not ultimately changed.

Interestingly, in a wild-type environment, the stringent pressure of type I IFN makes vhs RNase and deletion mutants indistinguishably feeble. The difference in pathogenicity between D215N and 333d41 became perceptible only in a less harsh environment, namely in IFN-$\alpha/\beta R^{-/-}$ mice. Our data support the possibility that there may be additional factors affecting the virulence of a RNase-deficient virus that retains vhs protein and suggest a more-cautious interpretation of the in vivo data. The heightened attenuation of the RNase-deficient mutant suggests the establishment of a cellular environment not encountered in cells infected with the virus that lacks vhs. This new environment makes the RNase-deficient virus less able to take advantage of lost cellular IFN responses. The results indicate that RNase activity is important for the virus but do not necessarily prove that it is the only contribution of vhs to virulence, because in some way, the presence of the enzymatically inactive protein creates a new hurdle for the virus to surmount.

The additional attenuation of a virus specifically lacking RNase activity over a virus lacking the vhs protein raises interesting questions about how the enzymatically inactive vhs mechanistically enhances attenuation. One possibility is that mutant vhs may bind cellular components of the translation initiation complex and, because it lacks enzymatic activity, essentially sequester the complex and prevent the cellular factors from recycling to initiate translation of viral messages. A second possible explanation for the slower replication and spread of the RNase-deficient virus in IFN-$\alpha/\beta R^{-/-}$ mice is that dominant negative effects of enzymatically inactive vhs may be exaggerated within the nervous system. Indeed, cell-type-specific differences in sensitivity to the shutoff activity of vhs within various neuronal cell populations have been observed (2, 43, 56) and may be related to variations in the levels of individual translation factors in different cells (24) as well as to MOIs (56). Of interest, the vhs-1 mutant of HSV-1 is RNase deficient yet reduces protein synthesis in cultured cerebellar granule neurons infected at a high MOI (2), suggesting a negative effect of enzymatically inactive vhs bound to translation initiation complexes. A RNase activity-deficient virus that lacks the capacity to form complexes with cellular translation initiation factors will be needed to address this possibility. Thus, vhs enzymatic activity may make two contributions to virulence, one by potentially degrading the mRNAs of critical host response factors of the type I IFN pathways and another by mechanically clearing translation initiation complexes of host messages so that viral proteins can be translated efficiently.

Our approach to the study of enzymatically inactive vhs extends a previous in vitro study performed with the vhs point mutant of HSV-1, vhs-1 (2), by examining effects in vivo. vhs-1 replicates poorly in cultures of mature mouse cerebellar neurons and induces fragmentation of the nuclei and DNA margination consistent with apoptotic cell death (2). These observations raise an intriguing third possibility: that vhs RNase activity may be involved in delaying or preventing apoptosis in neurons. By analogy to vhs-1, HSV-2 D215N may replicate inefficiently in the nervous system because it induces apoptotic cell destruction, resulting in delayed spread to and within neural tissues but eventual death of the mouse. Studies of apoptosis within the spinal cord after peripheral infection with the wild-type virus or D215N and 333d41 will be necessary to address this possibility. Understanding the mechanism underlying D215N attenuation will eventually provide further insight into the role(s) of vhs in HSV-2 pathogenesis.

## ACKNOWLEDGMENTS

This work was supported by award R01-AI057573 from the Public Health Service.

We thank Hong Wang and Mike Satzer for unflagging technical assistance. We are grateful to Tracy Smith and David Leib for providing the 333d41 virus and to Jim Smiley for providing us with viruses 333 and 333vhsB. Helpful discussions with Keril Blight, Mike Diamond, David Leib, Paul Olivo, Andy Pekosz, Pat Stuart, David Wang, Dong Yu, and members of their laboratories are greatly appreciated.

## REFERENCES

1. **Aubert, M., and J. A. Blaho.** 2001. Modulation of apoptosis during herpes simplex virus infection in human cells. Microbes Infect. **3:**859–866.
2. **Barzilai, A., I. Zivony-Elbom, R. Sarid, E. Noah, and N. Frenkel.** 2006. The herpes simplex virus type 1 vhs-UL41 gene secures viral replication by temporarily evading apoptotic cellular response to infection: Vhs-UL41 activity might require interactions with elements of cellular mRNA degradation machinery. J. Virol. **80:**505–513.
3. **Berthomme, H., B. Jacquemont, and A. Epstein.** 1993. The pseudorabies virus host-shutoff homolog gene: nucleotide sequence and comparison with alphaherpesvirus protein counterparts. Virology **193:**1028–1032.
4. **Cassady, K. A., M. Gross, and B. Roizman.** 1998. The second-site mutation in the herpes simplex virus recombinants lacking the $\gamma_1$34.5 genes precludes shutoff of protein synthesis by blocking the phosphorylation of eIF-2$\alpha$. J. Virol. **72:**7005–7011.
5. **Cassady, K. A., M. Gross, and B. Roizman.** 1998. The herpes simplex virus $U_S$11 protein effectively compensates for the $\gamma_1$34.5 gene if present before activation of protein kinase R by precluding its phosphorylation and that of the $\alpha$ subunit of eukaryotic translation initiation factor 2. J. Virol. **72:**8620–8626.
6. **Chou, J., J. J. Chen, M. Gross, and B. Roizman.** 1995. Association of a $M_r$ 90,000 phosphoprotein with protein kinase PKR in cells exhibiting enhanced phosphorylation of translation initiation factor e1F-2 $\alpha$ and premature shutoff of protein synthesis after infection with $\gamma_1$34.5$^-$ mutants of herpes simplex virus 1. Proc. Natl. Acad. Sci. USA **92:**10516–10520.
7. **Doepker, R. C., W.-L. Hsu, H. A. Saffran, and J. R. Smiley.** 2004. Herpes simplex virus virion host shutoff protein is stimulated by translation initiation factors eIF4B and eIF4H. J. Virol. **78:**4684–4699.
8. **Duerst, R. J., and L. A. Morrison.** 2007. Herpes simplex virus type 2-mediated disease is reduced in mice lacking RNase L. Virology **360:**322–328.
9. **Elgadi, M. M., and J. R. Smiley.** 1999. Picornavirus internal ribosome entry site elements target RNA cleavage events induced by the herpes simplex virus virion host shutoff protein. J. Virol. **73:**9222–9231.
10. **Elgadi, M. M., C. E. Hayes, and J. R. Smiley.** 1999. The herpes simplex virus vhs protein induces endoribonucleolytic cleavage of target RNAs in cell extracts. J. Virol. **73:**7153–7164.
11. **Everett, R. D., and M. L. Fenwick.** 1990. Comparative ONA sequence analysis of the host shutoff genes of different strains of herpes simplex virus: type 2 strain HG52 encodes a truncated UL41 product. J. Gen. Virol. **71:**1387–1390.
12. **Everly, D. N., Jr., P. Feng, I. S. Mian, and G. S. Read.** 2002. mRNA degradation by the virion host shutoff (Vhs) protein of herpes simplex virus: genetic and biochemical evidence that Vhs is a nuclease. J. Virol. **76:**8560–8571.
13. **Everly, D. N., Jr., and G. S. Read.** 1999. Site-directed mutagenesis of the virion host shutoff gene (UL41) of herpes simplex virus (HSV): analysis of functional differences between HSV type 1 (HSV-1) and HSV-2 alleles. J. Virol. **73:**9117–9129.

14. **Everly, D. N., Jr., and G. S. Read.** 1997. Mutational analysis of the virion host shutoff gene (UL41) of herpes simplex virus (HSV): characterization of HSV type 1 (HSV-1)/HSV-2 chimeras. J. Virol. **71:**7157–7166.
15. **Feng, P., D. N. Everly, Jr., and G. S. Read.** 2005. mRNA decay during herpes simplex virus (HSV) infections: protein-protein interactions involving the HSV virion host shutoff protein and translation factors eIF4H and eIF4A. J. Virol. **79:**9651–9664.
16. **Feng, P., D. N. Everly, Jr., and G. S. Read.** 2001. mRNA decay during herpesvirus infections: interaction between a putative viral nuclease and a cellular translation factor. J. Virol. **75:**10272–10280.
17. **Fenwick, M. L., and M. J. Walker.** 1978. Suppression of the synthesis of cellular macromolecules by herpes simplex virus. J. Gen. Virol. **41:**37–51.
18. **Geiss, B. J., J. E. Tavis, L. M. Metzger, D. A. Leib, and L. A. Morrison.** 2001. Temporal regulation of herpes simplex virus type 2 VP22 expression and phosphorylation. J. Virol. **75:**10721–10729.
19. **Goodbourn, S., L. Didcock, and R. E. Randall.** 2000. Interferons: cell signalling, immune modulation, antiviral response and virus countermeasures. J. Gen. Virol. **81:**2341–2364.
20. **Halford, W. P., L. A. Veress, B. M. Gebhardt, and D. J. Carr.** 1997. Innate and acquired immunity to herpes simplex virus type 1. Virology **236:**328–337.
21. **Haller, O., G. Kochs, and F. Weber.** 2006. The interferon response circuit: induction and suppression by pathogenic viruses. Virology **344:**119–130.
22. **He, B., M. Gross, and B. Roizman.** 1997. The $\gamma_1$34.5 protein of herpes simplex virus 1 complexes with protein phosphatase 1$\alpha$ to dephosphorylate the $\alpha$ subunit of the eukaryotic translation initiation factor 2 and preclude the shutoff of protein synthesis by double-stranded RNA-activated protein kinase. Proc. Natl. Acad. Sci. USA **94:**843–848.
23. **Heine, J. W., R. W. Honess, E. Cassai, and B. Roizman.** 1974. Proteins specified by herpes simplex virus. XII. The virion polypeptides of type 1 strains. J. Virol. **14:**640–651.
24. **Hernández, G., and P. Vazquez-Pianzola.** 2005. Functional diversity of the eukaryotic translation initiation factors belonging to eIF4 families. Mech. Dev. **122:**865–876.
25. **Jones, F. E., C. A. Smibert, and J. R. Smiley.** 1995. Mutational analysis of the herpes simplex virus virion host shutoff protein: evidence that vhs functions in the absence of other viral proteins. J. Virol. **69:**4863–4871.
26. **Knipe, D. M., and A. E. Spang.** 1982. Definition of a series of stages in the association of two herpesviral proteins with the cell nucleus. J. Virol. **43:**314–324.
27. **Kwong, A. D., and N. Frenkel.** 1987. Herpes simplex virus-infected cells contain a function(s) that destabilizes both host and viral mRNAs. Proc. Natl. Acad. Sci. USA **84:**1926–1930.
28. **Kwong, A. D., and N. Frenkel.** 1989. The herpes simplex virus virion host shutoff function. J. Virol. **63:**4834–4839.
29. **Lam, Q., C. A. Smibert, K. E. Koop, C. Lavery, J. P. Capone, S. P. Weinheimer, and J. R. Smiley.** 1996. Herpes simplex virus VP16 rescues viral mRNA from destruction by the virion host shutoff function. EMBO J. **15:**2575–2581.
30. **Leib, D. A.** 2002. Counteraction of interferon-induced antiviral responses by herpes simplex viruses. Curr. Top. Microbiol. Immunol. **269:**171–185.
31. **Leib, D. A., T. E. Harrison, K. M. Laslo, M. A. Machalek, N. J. Moorman, and H. W. Virgin.** 1999. Interferons regulate the phenotype of wild-type and mutant herpes simplex viruses in vivo. J. Exp. Med. **189:**663–672.
32. **Leib, D. A., M. A. Machalek, B. R. Williams, R. H. Silverman, and H. W. Virgin.** 2000. Specific phenotypic restoration of an attenuated virus by knockout of a host resistance gene. Proc. Natl. Acad. Sci. USA **97:**6097–6101.
33. **Livak, K. J., and T. D. Schmittgen.** 2001. Analysis of relative gene expression data using real-time quantitative PCR and the $2^{-\Delta\Delta}C_T$ method. Methods **25:**402–408.
34. **Lu, P., F. E. Jones, H. A. Saffran, and J. R. Smiley.** 2001. Herpes simplex virus virion host shutoff protein requires a mammalian factor for efficient in vitro endoribonuclease activity. J. Virol. **75:**1172–1185.
35. **Morrison, L. A., and D. M. Knipe.** 1996. Mechanisms of immunization with a replication-defective mutant of herpes simplex virus 1. Virology **220:**402–413.
36. **Morrison, L. A., X. J. Da Costa, and D. M. Knipe.** 1998. Influence of mucosal and parenteral immunization with a replication-defective mutant of HSV-2 on immune responses and protection from genital challenge. Virology **243:**178–187.
37. **Mossman, K. L.** 2002. Activation and inhibition of virus and interferon: the herpesvirus story. Viral Immunol. **15:**3–15.
38. **Mossman, K. L., H. A. Saffran, and J. R. Smiley.** 2000. Herpes simplex virus ICPO mutants are hypersensitive to interferon. J. Virol. **74:**2052–2056.
39. **Mossman, K. L., and J. R. Smiley.** 2002. Herpes simplex virus ICPO and ICP34.5 counteract distinct interferon-induced barriers to virus replication. J. Virol. **76:**1995–1998.
40. **Mukhopadhyay, A., G. E. Lee, and D. W. Wilson.** 2006. The amino terminus of the herpes simplex virus 1 protein Vhs mediates membrane association and tegument incorporation. J. Virol. **80:**10117–10127.
41. **Müller, U., U. Steinhoff, L. F. Reis, S. Hemmi, J. Pavlovic, R. M. Zinkernagel, and M. Aguet.** 1994. Functional role of type I and type II interferons in antiviral defense. Science **264:**1918–1921.
42. **Murphy, J. A., R. J. Duerst, T. J. Smith, and L. A. Morrison.** 2003. Herpes simplex virus type 2 virion host shutoff protein regulates alpha/beta interferon but not adaptive immune responses during primary infection in vivo. J. Virol. **77:**9337–9345.
43. **Nichol, P. F., J. Y. Chang, E. M. Johnson, Jr., and P. D. Olivo.** 1994. Infection of sympathetic and sensory neurons with herpes simplex virus does not elicit a shut-off of cellular protein synthesis: implications for viral latency and herpes vectors. Neurobiol. Dis. **1:**83–94.
44. **Oroskar, A. A., and G. S. Read.** 1989. Control of mRNA stability by the virion host shutoff function of herpes simplex virus. J. Virol. **63:**1897–1906.
45. **Pfaffl, M. W.** 2001. A new mathematical model for relative quantification in real-time RT-PCR. Nucleic Acids Res. **29:**e45.
46. **Read, G. S., and N. Frenkel.** 1983. Herpes simplex virus mutants defective in the virion-associated shutoff of host polypeptide synthesis and exhibiting abnormal synthesis of $\alpha$ (immediate early) viral polypeptides. J. Virol. **46:**498–512.
47. **Read, G. S., B. M. Karr, and K. Knight.** 1993. Isolation of a herpes simplex virus type 1 mutant with a deletion in the virion host shutoff gene and identification of multiple forms of the *vhs* (UL41) polypeptide. J. Virol. **67:**7149–7160.
48. **Schmelter, J., J. Knez, J. R. Smiley, and J. P. Capone.** 1996. Identification and characterization of a small modular domain in the herpes simplex virus host shutoff protein sufficient for interaction with VP16. J. Virol. **70:**2124–2131.
49. **Sciortino, M. T., B. Taddeo, M. Giuffre-Cuculletto, M. A. Medici, A. Mastino, and B. Roizman.** 2007. Replication-competent herpes simplex virus 1 isolates selected from cells transfected with a bacterial artificial chromosome DNA lacking only the $U_L$49 gene vary with respect to the defect in the $U_L$41 gene encoding host shutoff RNase. J. Virol. **81:**10924–10932.
50. **Smibert, C. A., B. Popova, P. Xiao, J. P. Capone, and J. R. Smiley.** 1994. Herpes simplex virus VP16 forms a complex with the virion host shutoff protein vhs. J. Virol. **68:**2339–2346.
51. **Smibert, C. A., and J. R. Smiley.** 1990. Differential regulation of endogenous and transduced $\beta$-globin genes during infection of erythroid cells with a herpes simplex virus type 1 recombinant. J. Virol. **64:**3882–3894.
52. **Smith, J. S., and N. J. Robinson.** 2002. Age-specific prevalence of infection with herpes simplex virus types 2 and 1: a global review. J. Infect. Dis. **186**(Suppl. 1)**:**S3–S28.
53. **Smith, T. J., C. E. Ackland-Berglund, and D. A. Leib.** 2000. Herpes simplex virus virion host shutoff (*vhs*) activity alters periocular disease in mice. J. Virol. **74:**3598–3604.
54. **Smith, T. J., L. A. Morrison, and D. A. Leib.** 2002. Pathogenesis of herpes simplex virus type 2 virion host shutoff (*vhs*) mutants. J. Virol. **76:**2054–2061.
55. **Strand, S. S., and D. A. Leib.** 2004. Role of the VP16-binding domain of vhs in viral growth, host shutoff activity, and pathogenesis. J. Virol. **78:**13562–13572.
56. **Strand, S. S., T. K. Vanheyningen, and D. A. Leib.** 2004. The virion host shutoff protein of herpes simplex virus type 1 has RNA degradation activity in primary neurons. J. Virol. **78:**8400–8403.
57. **Strelow, L. I., and D. A. Leib.** 1995. Role of the virion host shutoff (*vhs*) of herpes simplex virus type 1 in latency and pathogenesis. J. Virol. **69:**6779–6786.
58. **Su, Y. H., J. E. Oakes, and R. N. Lausch.** 1993. Mapping the genetic region coding for herpes simplex virus resistance to mouse interferon alpha/beta. J. Gen. Virol. **74:**2325–2332.
59. **Suzutani, T., M. Nagamine, T. Shibaki, M. Ogasawara, I. Yoshida, T. Daikoku, Y. Nishiyama, and M. Azuma.** 2000. The role of the UL41 gene of herpes simplex virus type 1 in evasion of non-specific host defense mechanisms during primary infection. J. Gen. Virol. **81:**1763–1771.
60. **Sydiskis, R. J., and B. Roizman.** 1966. Polysomes and protein synthesis in cells infected with a DNA virus. Science **153:**76–78.
61. **Taddeo, B., W. Zhang, and B. Roizman.** 2006. The $U_L$41 protein of herpes simplex virus 1 degrades RNA by endonucleolytic cleavage in absence of other cellular or viral proteins. Proc. Natl. Acad. Sci. USA **103:**2827–2832.
62. **Taddeo, B., M. T. Sciortino, W. Zhang, and B. Roizman.** 2007. Interaction of herpes simplex virus RNase with VP16 and VP22 is required for the accumulation of the protein but not for accumulation of mRNA. Proc. Natl. Acad. Sci. USA **104:**12163–12168.
63. **Walters, R. J., C. Rosenbaum, H. S. Willenberg, W. A. Scherbaum, and S. R. Bornstein.** 2002. Insulin, nerve growth factor and PACAP modulate the expression of $GABA_A$ subunits in PC12 cells. Neuroscience-Net http://www.neuroscience.com/manuscripts-2002/2002-001-walters/2002-001-walters.html.
64. **Xu, F., M. R. Sternberg, B. J. Kottiri, G. M. McQuillan, F. K. Lee, A. J. Nahmias, S. M. Berman, and L. E. Markowitz.** 2006. Trends in herpes simplex virus type 1 and type 2 seroprevalence in the United States. JAMA **296:**964–973.
65. **Zelus, B. D., R. S. Stewart, and J. Ross.** 1996. The virion host shutoff protein of herpes simplex virus type 1: messenger ribonucleolytic activity in vitro. J. Virol. **70:**2411–2419.